AD-A202 537

DTIC FILE COPY (2)

Unclassified

SECURITY CLASSIFICATION OF THIS PAGE (When Data Entered)

REPORT DOCUMENTATION PAGE		READ INSTRUCTIONS BEFORE COMPLETING FORM
1. REPORT NUMBER ARO 20850.3-EL	2. GOVT ACCESSION NO. N/A	3. RECIPIENT'S CATALOG NUMBER N/A
4. TITLE (and Subtitle) Analytic Distribution for Charge Carriers in a Semiconductor Dominated by Equivalent Intervalley Scattering		5. TYPE OF REPORT & PERIOD COVERED Technical 6. PERFORMING ORG. REPORT NUMBER
7. AUTHOR(s) Gregory K. Schenter and Richard L. Liboff		8. CONTRACT OR GRANT NUMBER(s) DAAG 29-84-K-0093
9. PERFORMING ORGANIZATION NAME AND ADDRESS Cornell University, Ithaca, NY 14853		10. PROGRAM ELEMENT, PROJECT, TASK AREA & WORK UNIT NUMBERS
11. CONTROLLING OFFICE NAME AND ADDRESS U.S. Army Research Office P.O. Box 12211, Research		12. REPORT DATE October 10, 1988 13. NUMBER OF PAGES 34
14. MONITORING AGENCY NAME & ADDRESS (if different from Controlling Office)		15. SECURITY CLASS. (of this report) Unclassified 15a. DECLASSIFICATION/DOWNGRADING SCHEDULE
16. DISTRIBUTION STATEMENT (of this Report) Approved for public release; distribution unlimited		
17. DISTRIBUTION STATEMENT (of the abstract entered in Block 20, if different from Report) N/A		
18. SUPPLEMENTARY NOTES The views, opinions, and/or findings in this report are those of the authors and should not be construed as an official Dept. of the Army position, policy, or decision, unless so designated by other documentation.		
19. KEY WORDS (Continue on reverse side if necessary and identify by block number) High-Field Transport; Semiconductor; Equivalent Intervalley; Uehling-Uhlenbeck equation; Drift velocity; Silicon; Strain-Acoustic		
20. ABSTRACT (Continue on reverse side if necessary and identify by block number) (see reverse side)		

DD FORM 1473 1 JAN 73 EDITION OF 1 NOV 65 IS OBSOLETE

S/N 0102-014-6601

SECURITY CLASSIFICATION OF THIS PAGE (When Data Entered)

The transport of charge carriers in Silicon immersed in an electric field is studied using the quasiclassical Uehling-Uhlenbeck equation. Strain-acoustic and equivalent intervalley electron-phonon interactions are taken into account. A nonlinear difference-differential equation for the distribution function of charge carriers is obtained. An approximate analytic solution to this equation is constructed from which an expression for drift velocity is derived. Comparison with values obtained from this expression is found to give very good agreement with experimental measurement for electric fields up to 10^5 V/cm.

100,000

Table of Contents

I. INTRODUCTION

In recent works by the authors[1,2] the problem of charge-carrier transport in a semiconductor in the presence of an applied electric field was examined. A new nonlinear differential equation for the distribution function of charge carriers was derived incorporating acoustic-strain interactions and solved exactly. In the present work this analysis is extended to include equivalent intervalley scattering which is significant to transport processes in Silicon.[3,4] The analysis considers only single phonon interactions. Furthermore, charge-carrier energy is sufficiently small so that non-equivalent intervalley transitions are omitted. Again a differential equation is derived for the distribution of charge carriers as function of energy. However, in the present case, this equation includes "difference" terms stemming from intervalley scattering. An approximate solution to this equation is obtained in the following manner. As a first step, a group of difference terms is approximated by a differential form whose components are motivated through matching with correct asymptotic solutions. The resulting nonlinear equation is solved exactly thus yielding an approximate solution to the original equation.

In the second step this approximate solution is employed in constructing a solution to the full nonlinear difference-differential equation. The resulting distribution appears as a piecewise continuous function separated at the intervalley phonon energy. The solution so obtained shows very good agreement with results generated by a Monte Carlo analysis of the problem. The new analytic distribution is used to obtain a closed expressions for drift velocity as function of applied electric field, charge-carrier density and temperature.

Comparison of these results with experimental values is found to give very good agreement for n-type Silicon at room temperature and fields up to 10^5 V/cm.

II. ANALYSIS

A. Starting Equations

In this work we consider the following generalized Uehling Uhlenbeck[5,6] equation for the distribution function, $f(\underset{\sim}{k},t)$,

$$\frac{\partial f}{\partial t} + \frac{e\underset{\sim}{E}}{\hbar} \cdot \frac{\partial f}{\partial \underset{\sim}{k}} = \hat{J}_{SA}(f) + \hat{J}_{IV}(f) \tag{1}$$

where $\hat{J}_{SA}$ represents charge carrier - strain acoustic interactions and $\hat{J}_{IV}$ represents equivalent intervalley interactions. Electric field and particle momentum are denoted by $\underset{\sim}{E}$ and to $\underset{\sim}{k}$, respectively. Both collision terms are of the form

$$\hat{J}_{\alpha}(f) = \sum_{\underset{\sim}{k}'} [f'(1-af)\, S^{(\alpha)}_{\underset{\sim}{k}'\underset{\sim}{k}} - f(1-af')\, S^{(\alpha)}_{\underset{\sim}{k}\underset{\sim}{k}'}] \tag{2}$$

where $f' \equiv f(\underset{\sim}{k}')$, etc. and $S^{(\alpha)}_{\underset{\sim}{k}'\underset{\sim}{k}}$ represents the scattering from the state $\underset{\sim}{k}'$ to $\underset{\sim}{k}$ due to the mechanism α. The bookkeeping parameter a has the value 1 and may be set equal to zero in the classical domain. In writing (2) we have assumed the normalization

$$\sum_{\underset{\sim}{k}} f(\underset{\sim}{k}) = N \tag{3a}$$

In the continuum limit this relation becomes

$$\frac{V}{(2\pi)^3} \int f(\underset{\sim}{k})\, d\underset{\sim}{k} = N \tag{3b}$$

where V is crystal volume.

In this analysis we will concentrate on the transport of charge carriers in Silicon. The possible phonon-charge carrier interactions for this case are shown in Fig. 1. It is assumed that charge-carrier energy is sufficiently small ($\lesssim$ 1 eV) thereby permitting us to neglect non-equivalent intervalley scattering.[7] In this diagram "S" denotes "strain" (often refered to as "deformation potential"), O and A represent "optical" and "acoustic" phonons, respectively. In Silicon there are two possible intervalley (IV) transitions denoted by g (parallel valleys) and f (perpendicular valleys). The terms T and L refer to transverse and longitudinal phonons, respectively.

To determine the relative importance of scattering mechanisms we define the total scattering rate

$$\lambda^{(\alpha)}_{\underset{\sim}{k}} = \sum_{\underset{\sim}{k}'} S^{(\alpha)}_{\underset{\sim}{k}\,\underset{\sim}{k}'} \tag{4}$$

These rates are calculated in Appendix A and are sketched in Fig. 2 relevant to Silicon at 300°K. It is evident from these figures that the interactions g (LO±) and (SA±) dominate thereby justifying the RHS of (1). In this notation (+) refers to phonon absorption and (-) to phonon emission. It should be noted that the SO interaction listed in Fig. 1 does not appear in the rate calculations of Fig. 2. This is attributed to symmetry properties of the crystal which in turn disallow this transition.[4,8]

B. Reduction of Kinetic Equation

To account for anisotropy of the distribution function we introduce the expansion[9]

$$f(\underset{\sim}{k},t) = \sum_{\ell} f_{\ell}(\mathcal{E},t)\; P_{\ell}(\mu) \tag{5a}$$

where

$$\mathcal{E} \equiv \frac{\hbar^2 k^2}{2m} \quad , \qquad \mu \equiv \hat{\underset{\sim}{E}}\cdot\hat{\underset{\sim}{k}} \tag{5b}$$

Hatted **variables** are unit vectors and m is effective mass. Note that in writing (5b) the constant energy surface has been approximated by a sphere. Going to equilibrium and keeping only the first two terms in (3) we obtain

$$\frac{e\underset{\sim}{E}}{\hbar} \cdot \frac{\partial f}{\partial \underset{\sim}{k}} = eE\sqrt{\frac{2}{m\ell}}\left[\frac{1}{3}\frac{\partial}{\partial \ell}(\ell f_1) + \mu\ell\frac{\partial}{\partial \ell}f_o\right] \qquad (6)$$

For J_{SA} we obtain[2]

$$\begin{aligned}\hat{J}_{SA}(f) &= \hat{J}_{SA}(f_o) - \frac{\mu}{\tau_{SA}}f_1 \\ &= \frac{1}{l}\sqrt{\frac{2}{m\ell}}\left\{\frac{2mu^2}{k_BT}\frac{\partial}{\partial \ell}\left[\ell^2\,\hat{g}(f_o)\right] - \mu\ell f_1\right\}\end{aligned} \qquad (7)$$

where the relaxation time τ_{SA} is as implied and [1]

$$\hat{g}(f_o) \equiv k_BT\frac{\partial f_o}{\partial \ell} + f_o(1 - af_o) \qquad (7a)$$

Acoustic mean free path, l, is given by [1,3]

$$l = \frac{\pi\hbar^4\rho u^2}{m^2E_1^2\;k_BT} \qquad (7b)$$

In this expression ρ is crystal mass density, u is acoustic phonon velocity, T is crystal temperature and E_1 is the deformation potential constant. In obtaining (7) it was assumed that

$$\hbar uq << k_BT \qquad (8)$$

where $\underset{\sim}{q}$ is phonon wavevector. For $\hat{J}_{IV}(f)$ we obtain (see Appendix B)

$$\begin{aligned}\hat{J}_{IV}(f) = \sum_{\pm}\alpha_{\pm}\Big[&\bar{f}_o(1 - af_o - a\mu f_1)(n_{IV} + \tfrac{1}{2} \pm \tfrac{1}{2}) \\ &- (f_o + \mu f_1)(1 - a\bar{f}_o)(n_{IV} + \tfrac{1}{2} \mp \tfrac{1}{2})\Big]\end{aligned} \qquad (9)$$

where the sum is over upper and lower terms in the summand and are associated with phonon emission and absorption. Furthermore

$$\alpha_{\pm} \equiv \frac{1}{\ell_{IV}} \sqrt{\frac{2(\mathcal{E} \pm \hbar\omega_{IV})}{m}}\ \theta\ (\mathcal{E} \pm \hbar\omega_{IV}) \tag{9a}$$

Here we have introduced

$$\begin{aligned} \theta(x) &= 1, \ x \geq 0 \\ \theta(x) &= 0, \ x < 0 \end{aligned} \tag{9b}$$

The displaced distribution is given by

$$\bar{f}_o(\mathcal{E}) = f_o(\mathcal{E} \pm \hbar\omega_{IV}) \tag{9c}$$

and the length ℓ_{IV} is written for

$$\ell_{IV} = \frac{2\rho\omega_{IV}\pi\hbar^3}{D^2 m^2} \tag{9d}$$

where D is the intervalley interaction constant (in units of energy/length).[3,4] Intervalley phonon frequency is written ω_{IV}. The intervalley phonon density is taken to be

$$n_{IV} = \frac{1}{\exp\left[\frac{\hbar\omega_{IV}}{k_B T}\right] - 1} \tag{9e}$$

Note that (9) has the structure

$$\hat{J}_{IV}(f) = \hat{J}_{IV}(f_o) - \frac{\mu}{\tau_{IV}} f_1 \tag{10}$$

$$\hat{J}_{IV}(f) = \sum_{\pm} \alpha_{\pm} \{[\bar{f}_o(n_{IV} + \tfrac{1}{2} \pm \tfrac{1}{2}) - f_o(n_{IV} + \tfrac{1}{2} \mp \tfrac{1}{2} \pm a\, \bar{f}_o)]$$

$$- \mu\, f_1(n_{IV} + \tfrac{1}{2} \mp \tfrac{1}{2} \pm a\, \bar{f}_o)\} \tag{10a}$$

where again τ_{IV} is as implied. Inserting (6,7,10) in (1) and equating Legendre coefficients we obtain

$$\frac{1}{3} \frac{\partial}{\partial \mathcal{E}} (\mathcal{E} f_1) = \frac{2mu^2}{eE\ell} \frac{1}{k_B T} \frac{\partial}{\partial \mathcal{E}} [\mathcal{E}^2\, \hat{g}(f_o) \tag{11a}$$

$$+ \sum_{\pm} \frac{1}{eE} \sqrt{\frac{m\mathcal{E}}{2}}\, \alpha_{\pm} [\bar{f}_o(n_{IV} + \tfrac{1}{2} \pm \tfrac{1}{2}) - f_o(n + \tfrac{1}{2} \mp \tfrac{1}{2} \pm a\, \bar{f}_o)]$$

$$\mathcal{E} \frac{2f_o}{\partial \mathcal{E}} = - \frac{\mathcal{E}}{eE\ell} f_1 - \sum_{\pm} \frac{1}{eE} \sqrt{\frac{m\mathcal{E}}{2}}\, \alpha_{\pm}(n_{IV} + \tfrac{1}{2} \mp \tfrac{1}{2} \pm a\, \bar{f}_o)\, f_1 \tag{11b}$$

Eliminating f_1 from (11a,b) and introducing the nondimensional energy

$$x \equiv \mathcal{E}/k_B T \tag{12}$$

gives the desired nonlinear difference-differential equation

$$(\phi f_o')' + [x^2\, \hat{g}(f_o)]' + \sum_{\pm} \zeta_{\pm} [\bar{f}_o(n_{IV} + \tfrac{1}{2} \pm \tfrac{1}{2})$$

$$- f_o(n_{IV} + \tfrac{1}{2} \mp \tfrac{1}{2} \pm a\, \bar{f}_o)] = 0 \tag{13}$$

where prime denotes differentiated with respect to x. Furthermore

$$\phi \equiv \frac{sx^2}{x + \xi_+ + \xi_-}$$

$$\xi_{\pm} \equiv r(n_{IV} + \tfrac{1}{2} \mp \tfrac{1}{2} \pm a\, \bar{f}_o)\, \sqrt{x(x \pm \Delta)}\; \theta(x \pm \Delta) \tag{14}$$

$$\zeta_{\pm} \equiv r\tau\, \sqrt{x(x \pm \Delta)}\; \theta(x \pm \Delta)$$

In the proceeding we have introduced the dimensionless constants

$$r \equiv \ell/\ell_{IV} \ , \ \Delta \equiv \frac{\hbar\omega_{IV}}{k_B T} \ , \ \tau \equiv \frac{k_B T}{2mu^2}$$

and dimensionless electric field[3,8]

$$\mathcal{E} \equiv \frac{(eE\ell)^2}{6mu^2 k_B T} \equiv \left(\frac{E}{E^*}\right)^2 \qquad (15b)$$

Note in particular that setting $r = 0$ in (13) has the effect of shutting off intervalley scattering.

With these parameters given by (15), solving (11b) for f_1 and inserting the result into (5a) gives

$$f(x,\mu) = \left[1 - \mu \frac{eE\ell}{k_B T} \left(\frac{x}{x + \xi_+ + \xi_-}\right) \frac{\partial}{\partial x}\right] f_o(x) \qquad (16)$$

The noramlization (3b) assumes the following form when written in terms of the nondimensional energy x:

$$\int f_o(x)\sqrt{x}dx = \frac{\sqrt{\pi}}{2} \Lambda \qquad (17)$$

where Λ is the quantum degenerary parameter[10]

$$\Lambda = n_c \lambda_d{}^3 \qquad (17a)$$

and λ_d is the thermal deBroglie wavelength

$$\lambda_d{}^2 = \frac{2\pi\hbar^2}{mk_B T} \qquad (17b)$$

and n_c denotes charge carrier denisties. Some typical values of these parameters[4] are displayed in Table 1.

C. Limiting Properties

We wish to consider solution to (13) in three limiting cases:

(a) $r = 0$

Thus has the effect of turning off intervalley interactions (i.e., $\ell_{IV} \to \infty$). In this event (13) reduces to

Table 1

Values of Physical Constants

Used in This Analysis

material	n-type Si
T	$300^{\circ}K$
Δ	2.40
n_{IV}	0.100
γ	85.5
r	1.65
E^{*}	497 V/cm
$m = \sqrt[3]{m_{\parallel} m_{\perp}{}^{2}}$	$0.33m_{e}$
E_{1}	5.0 eV
D	11.0×10^{8} eV/cm
$\hbar\omega_{IV}$	0.06 eV

$$(sxf_o')' + [x^2\hat{g}(f_c)]' = 0 \tag{18}$$

whose solution was studied in detail in reference 1 and is given by

$$f_{SL}(x) = \frac{1}{a + Be^x\left(\frac{s}{s+x}\right)^s} \tag{19}$$

where B is a normalization constant.

(b) s = 0

This limit corresponds to turning off the applied electric field. There results

$$[x^2\,\hat{g}(f_o)]' + \sum_{\pm} \hat{c}_{\pm}(f_o) = 0 \tag{20}$$

where

$$\hat{c}_{\pm}(f_o) \equiv \zeta_{\pm}\,[\bar{f}_o(n_{IV} + \tfrac{1}{2} \pm \tfrac{1}{2}) - f_o(n_{IV} + \tfrac{1}{2} \mp \tfrac{1}{2} \pm a\bar{f}_o)] \tag{20a}$$

A physically relevant solution to (20) is given by the Fermi-Dirac distr bution

$$f_{FD}(x) = \frac{1}{a+Be^x} \tag{21}$$

Note in particular that

$$\hat{g}(f_{FD}) = \hat{c}_+(f_{FD}) = \hat{c}_-(f_{FD}) = 0 \tag{21a}$$

(c) $\Delta \to 0$

This limit corresponds to $\hbar\omega_{IV} << k_BT$. In this limit we find

$$n_{IV} = \frac{1}{\Delta} - \frac{1}{2} + O(\Delta) \tag{22a}$$

$$\bar{f}_o = f_o \pm \Delta f_o' + O(\Delta^2) \tag{22b}$$

in which case

$$\hat{C}_{\pm}(f_o) = \zeta_{\pm}\{\pm\, \hat{g}(f_o) + \frac{\Delta}{2}\, [\hat{g}(f_o)]' + O(\Delta^2)\} \tag{23b}$$

Furthermore, with $\theta(x \pm \Delta) \to 1$ we find

$$\zeta_{\pm} = r\gamma(x \pm \frac{\Delta}{2}) + O(\Delta^2) \tag{23c}$$

Combining these results gives

$$\hat{C}_{\pm}(f_o) = \pm\, r\gamma x\, \hat{g}(f_o) + \frac{1}{2}\, [r\gamma x\Delta\, \hat{g}(f_o)]' + O(\Delta^2) \tag{23d}$$

Thus

$$\sum_{\pm} \hat{C}_{\pm}(f_o) = [r\gamma x\Delta\, \hat{g}(f_o)]' + O(\Delta^2) \tag{23e}$$

Furthermore

$$\xi_{\pm} = \frac{rx}{\Delta} \pm \frac{r}{2}\, [\,1 - x(1 - 2a\, f_o)] + O(\Delta) \tag{23f}$$

which gives

$$\varphi(x) = \frac{sx}{1 + \frac{2r}{\Delta} + O(\Delta)} \tag{23g}$$

Substituting these results into (13) converts it to the following perfect differential equation:

$$\left[\frac{s\ x\ f_o'}{1 + \frac{2r}{\Delta}}\right]' + [x^2\ g(f_o)]' + [r\gamma\Delta x\ g(f_o)]' = 0 \tag{24}$$

Integrating we obtain (relevant to $\Delta \ll 1$)

$$f_o(x) = \frac{1}{a + B\ e^{x}\left(\frac{s'}{x + r\gamma\Delta}\right)^{s'}} \tag{25}$$

where

$$s' \equiv \frac{s}{1 + \frac{2r}{\Delta}} \tag{25a}$$

These limiting solutions will come into play in constructing a solution to (13).

III. APPROXIMATE ANALYTIC SOLUTION

A. Integration Technique

To convert (13) to a more tractable form we write (deleting the subscript on f_o)

$$\Sigma_{\pm}\ \hat{C}_{\pm}(f) = [\psi(x)\ \hat{g}(F)]' + \kappa(x) \qquad (26)$$

Note that the lead terms in this approximation maintains the property (21a) and is consistent with the finding given by (23e). The trial function $\psi(x)$ which also contains arbitrary parameters is constructed in a manner which effectively minimizes the error term κ. Having thus constructed ψ, a solution to (13) is then obtained in which κ is neglected.

B. Approximate Solution

We now consider the solution to the complete equation (13) with the approximation (26) and $\kappa = 0$.

$$(\phi f')' + [x^2\ \hat{g}(f)]' + [\psi\ \hat{g}(f)]' = 0 \qquad (27)$$

where, we recall, ψ is an arbitrary function to be determined and ϕ as given by (14) depends on f. Integrating (27) gives

$$(\phi + x^2 + \psi)f' + (x^2 + \psi)f(1 - af) = C_1 \qquad (28)$$

where C_1 is a constant. This equation may be further integrated provided ϕ is weakly dependent on f. This is the case when $af \ll n_{IV}$. In the classical domain where $a = 0$, this condition is trivially satisfied. In the quantum domain ($a = 1$) this condition become $f \ll n_{IV}$ which is compatible with the property $f < 1$ and the fact that the distribution n_{IV} relevant to bosons, may be greater than 1.

Assuming this constraint is satisfied and selting $C_1 = 0$, we obtain

$$f_\psi(x) = \frac{1}{a + B \exp \left[x - \int_0^x \left[\frac{\phi_o(y)}{\phi_o(y) + y^2 + \psi(y)}\right] dy\right.} \tag{29}$$

where ϕ_o equals ϕ with $a = 0$.

C. <u>Full Solution</u>

With the $f_\psi(x)$ as given by (29) at hand we now seek to determine the solution to (13), $f(x)$. To these ends the LHS of (13) is rewritten

$$\hat{L}(f) \equiv (\phi f')' + [x^2 \hat{g}(f)]' + \sum_{\pm} \hat{C}_\pm(f) \tag{30}$$

and we consider the functional

$$\Gamma[f] \equiv \int_0^\infty [\hat{L}(f)]^2 \, dx \geq 0 \tag{31}$$

where the equality corresponds to the solution to (13). The final form of $f(x)$ is determined by minimizing $\Gamma[f]$ or, equivalently, by finding f such that

$$\delta \, \Gamma[f] = 0 \tag{32}$$

where δ is a variation with respect to f.

Motivated by the results (23 c, e) relevant to case c, $(\Delta \rightarrow 0)$, we set

$$\psi = b \, \zeta_+ + (\Delta - b) \, \zeta_- \tag{33}$$

which at $b = \Delta/2$, and recalling (26), returns the asymptotic form (23e), i.e., $\psi = r\gamma\Delta x$.

Numerical attempts at solving (32) at $\Lambda << 1$ strongly suggest that the solution be separated into two components corresponding to $x < \Delta$ and $x > \Delta$. The resulting form is given by

$$f(x) = \begin{bmatrix} c\, f_\psi(x) + (1 - c)\ [f_\psi(\Delta) + f_\psi'(\Delta)(x - \Delta)],\ x < \Delta \\ f_\psi(x), \quad x > \Delta \end{bmatrix} \tag{34}$$

which is seen to be continuous at $x = \Delta$. With (33) and (34) we find that the functional, $\Gamma[f]$, becomes a function of the parameters (b,c). The conditions (32) then becomes

$$\frac{\partial\Gamma}{\partial b} = \frac{\partial\Gamma}{\partial c} = 0 \tag{35}$$

Solutions to these equations determine b and c as functions of the parameters (T, Λ, s).

As we wish to compare final results with experiment, this procedure was carried out for n-type Silicon at $300^{\circ}K$ with $\Lambda << 1$. Resulting values of b and c vs electric field, s, are shown in Fig. 3.

Approximate analytic expessions describing these values are given by

$$b(s) = \theta(s-480)\ \log_{10}\left(\frac{s}{58}\right)^{0.81} + 0.74\ \theta(480 - s) \tag{36a}$$

$$c(s) = \frac{1}{2}\ \{1 - \tanh\ [\log_{10}\left(\frac{s}{24}\right)^{1.3}]\} \tag{36b}$$

Characteristic behavior of these curves at small and large s is due to the following. From (14) we, note that $\phi(x) \propto s$. Thus at small s, recalling (29) we see that $f_\psi(x)$ grows insensitive to $\psi(x)$, and therefore to b. This property was confirmed in numerical analysis where it was observed that $\partial^2\Gamma/\partial b^2 \simeq 0$ in the domain $s \lesssim 100$.

Concerning c(s), it was shown that the solution to the principal equation (13) goes to the Fermi-Dirac distribution as $s \to 0$. Thus with reference to (34) we see that this behavior corresponds to $c \to 1$. For large s, one expects the component $f(x > \Delta)$ to dominate in (34). As this component does not contain c, again one finds $\partial^2\Gamma/\partial c^2 \simeq 0$ in this domain (i.e., $s \gtrsim 100$).

With these values of b(s) and c(s) at hand the distribution f(x) as given by (34) is plotted for various values of s in Fig. 4. From these curves it is evident that $f(x \gtrsim 40)$ (corresponding to $\mathcal{E} \gtrsim 1\text{eV}$) is vanishingly small. This is consistent with our omission of non-equivalent intervalley scattering.

D. <u>Drift Velocity</u>

With the normalization of $f(\underset{\sim}{k})$ as given by (3) we write

$$\underset{\sim}{v}_d = \langle \underset{\sim}{v} \rangle = \frac{1}{n_c} \int \frac{\hbar \underset{\sim}{k}}{m} f(\underset{\sim}{k}) \frac{d\underset{\sim}{k}}{(2\pi)^3} \qquad (37)$$

Converting to integration over x and μ, and recalling (16) we obtain

$$\underset{\sim}{v}_d = -\frac{4}{\sqrt{3\pi}} \frac{u\sqrt{s}\,\hat{\underset{\sim}{E}}}{\Lambda} \int_0^\infty \frac{x^2}{x + \xi_+ + \xi_-} \frac{df_o}{dx} dx \qquad (38)$$

In obtaining (38) we employed the tensor relation

$$\int \hat{\underset{\sim}{k}}\hat{\underset{\sim}{k}}\, dk = \frac{\hat{\underset{\sim}{E}}}{3} \int d\underset{\sim}{k} \qquad (38a)$$

(recall $\mu = \hat{\underset{\sim}{E}} \cdot \hat{\underset{\sim}{k}}$).

Integrating (38) by parts gives the final form (with $\xi \equiv \xi_+ + \xi_-$)

$$\underset{\sim}{v}_d = \frac{4}{\sqrt{3\pi}} \frac{u\sqrt{s}\hat{\underset{\sim}{E}}}{\Lambda} \int_0^\infty f(x) \frac{d}{dx} \left(\frac{x^2}{x + \xi}\right) dx \qquad (39)$$

where, we recall, $f(x) \equiv f_o(x)$ is given by (34). A plot of (39) for n-type Silicon at 300^oK and $\Lambda \ll 1$, as a function of electric field E, is given in Fig. 5. A compilation of experimental results[11] is drawn on the same graph. It should be emphasized that this agreement with experiment in no way depends on the fitting of free parameters.

IV. COMPARISION OF ANALYTIC AND MONTE CARLO RESULTS

As a self consistent check of the solution (34) we re-evaluated the solution numerically employing a Monte Carlo technique such as described in reference 4. Numerical values of parameters used in this analysis are given in Table 1. The analysis addresses the steady-state solution of (1) with $a = 0$ and scattering rates described in Appendix A. In this procedure we obtain $f(\varepsilon,\mu)$. The $\ell = 0$ component of (5a) is then given by

$$f_o(\varepsilon) = \frac{1}{2}\int_{-1}^{1} d\mu \; f(\varepsilon,\mu) \tag{40}$$

A plot of $f_o(\varepsilon)$ so obtained for the specific case $s = 100$ is compared with our analytic result (34) and is shown in Fig. 6. The discreteness of the Monte Carlo result is due to the finite mesh in energy whereas the fluctuations of the results are due to the statistical nature of the numerical procedure. The Monte Carlo curve shown corresponds to a sample of 10,000 collisions.

V. CONCLUSIONS

A nonlinear difference-differential equation for the distribution of charge carriers in a semiconducter including strain acoustic and equivalent intervalley scattering was derived. Introducing an approximate differential form for one term in this equation permitted exact solution. This solution was then used in tandem with a numerical analysis to obtain an approximate solution to the original equation in the near-classical domain. The distribution so obtained was applied in evaluation of drift velocity for n-type Silicon at room temperature. Results were found to be in very good agreement with measured values for electric fields up to 10^5 V/cm.

IV. ACKNOWLEDGEMENTS

This research was supported in part by contract DAAG 29-84-K-0093 with the United States Army Research Office and in part by the Mathematical Sciences Institute of Cornell University.

Appendix A

Scattering Rates

In this appendix we calculate the scattering rates $S_{\underset{\sim}{k}\underset{\sim}{k}'}$ that appear in our starting equation (2) and the net rates $\lambda^{(\alpha)}_{\underset{\sim}{k}}$ given by (4).

For SA interactions we write

$$S^{(SA\pm)}_{\underset{\sim}{k}\underset{\sim}{k}'} = \frac{2\pi}{\hbar} \left(\frac{E_1^2\hbar}{2V\rho u}\right) q \left[n_{SA}(q) + \frac{1}{2} \mp \frac{1}{2}\right] \delta(\mathcal{E}' - \mathcal{E} \mp \hbar uq) \quad \text{(A1)}$$

where upper and lower signs refer, respectively, to phonon absorption and emission. Furthermore

$$\pm \underset{\sim}{q} = \underset{\sim}{k}' - \underset{\sim}{k}$$

represents phonon wavevector and

$$n_{SA}(q) = \frac{1}{\exp\left(\frac{\hbar uq}{k_B T}\right) - 1} \simeq \frac{k_B T}{\hbar uq} - \frac{1}{2} \quad \text{(A2)}$$

where we have recalled the approximation (8). For IV interactions we write [3,4,8]

$$S^{(IV\pm)}_{\underset{\sim}{k}\underset{\sim}{k}'} = \frac{2\pi}{\hbar} \left(\frac{D^2\hbar}{2V\rho\omega_{IV}}\right) \left(n_{IV} + \frac{1}{2} \mp \frac{1}{2}\right) \delta(\mathcal{E}' - \mathcal{E} \mp \hbar\omega_{IV}) \quad \text{(A3)}$$

For the net scattering rates (4), with (3b) we write

$$\lambda^{(\alpha)}_{\underset{\sim}{k}} = V \int S^{(\alpha)}_{\underset{\sim}{k}\underset{\sim}{k}'} \frac{d\underset{\sim}{k}'}{(2\pi)^3} \quad \text{(A4)}$$

Inserting the preceeding expressions and integrating we obtain

$$\lambda^{(SA\pm)}_{\underset{\sim}{k}} = \frac{mE_1^2}{4\pi\hbar^2\rho u} \frac{1}{k} \left[\frac{k_B T}{\hbar u} \frac{(2k\pm 2mu/\hbar)^2}{2} \mp \frac{1}{2} \frac{(2k\pm 2mu/\hbar)^3}{3}\right] \quad \text{(A5)}$$

and

$$\lambda_{\underset{\sim}{k}}^{(IV\pm)} = \frac{mD^2}{2\pi\hbar^2\rho\omega_{IV}} \frac{\sqrt{2m}}{\hbar} \sqrt{\varepsilon \pm \hbar\,\omega_{IV}}\,\theta(\varepsilon \pm \hbar\omega_{IV})\ (n_{IV} + \tfrac{1}{2} \mp \tfrac{1}{2})$$

$$= \alpha_{\pm}\ (n_{IV} + \tfrac{1}{2} \mp \tfrac{1}{2}) \tag{A6}$$

where $\alpha_{\pm}$ is given by (9a).

Appendix B

Intervalley Collision Integral

In this appendix we wish to obtain the intervalley collision integral $\hat{J}_{IV}$ given by (9). Combining (2) and (A3) together with the limiting process (3a) gives

$$\hat{J}_{IV}(f) = V \int \frac{d\underset{\sim}{k}'}{(2\pi)^3} \sum_{\pm} \frac{2\pi}{\hbar} \frac{\hbar\ D^2}{2V\rho\omega_{IV}}\ \delta(\varepsilon' - \varepsilon \mp \hbar\omega_{IV})$$

$$[f'(1 - af)\ (n_{IV} + \tfrac{1}{2} \pm \tfrac{1}{2}) - f(1 - af')\ (n_{IV} + \tfrac{1}{2} \mp \tfrac{1}{2})] \tag{B1}$$

Now we note

$$d\underset{\sim}{k}' = \frac{(2m)^{3/2}}{2\hbar^3} \sqrt{\varepsilon'}\ d\varepsilon' d\mu' d\phi' \tag{B2}$$

where with (5b)

$$\mu' = \hat{\underset{\sim}{k}}' \cdot \hat{\underset{\sim}{E}} \tag{B3}$$

and ϕ is an azimuthal angle about the E axis. Furthermore

$$f' \equiv f_o(\varepsilon') + \mu' f_1(\varepsilon') \tag{B4}$$

With

$$\int d\mu' = 2 \quad , \quad \int d\mu'\mu' = 0$$

and recalling $\alpha_\pm$ given by (9a), integration over $\mathcal{E}'$ returns (9). Note in particular that the difference terms $\bar{f}_o$ in (9) stem from the delta function in (B1).

References

1. R.L. Liboff and G.K. Schenter, Phys. Rev B 34, 7063 (1986).
2. G.K. Schenter and R.L. Liboff, J. Appl. Phys. 62, 177 (1987).
3. E.M. Conwell, High Field Transport in Semiconductors, Solid State Physics edited by F. Seitz, D. Turnbull and H. Ehrenreich (Acedemic, New York, 1967), Vol. 9, Suppl.
4. Hot Electron Transport in Semiconductors, edited by L. Reggiani (Springer, New York, 1985).
5. E.A. Uehling and G.E. Uhlenbeck, Phys Rev 43, 552 (1933).
6. R.L. Liboff, Kinetic Theory: Classical Quantum and Relativistic Descriptions, (Prentice Hall, Englewood Cliffs, NJ, 1988).
7. J.R. Chelikowsky and M.L. Cohen, Phys Rev B 14, 556 (1976).
8. B.R. Nag, Theory of Electron Transport in Semiconductors (Pergamon, New York, 1972).
9. W.P. Allis, Handbuch der Physik (Springer, Berlin, 1955).
10. R.L. Liboff, J. Appl. Phys 58, 4438 (1985).
11. C. Jacoboni, C. Canali, G. Ottaviani and A. Alberigi Quarauta, Solid State Electronics 20, 77 (1977).

Figure Captions

1. Diagram illustrating electron-phonon interactions relevant to Silicon. Notation is defined in the text.

2. Scattering rates in n-type Silicon at 300°K. (a) Strain-acoustic (SA) and g intervalley scattering. (b) f intervalley scattering. Absorption and emission are referred to as (+/-) respectively whereas longitudinal and transverse are referred to as L and T respectively. Each curve for $\lambda_{\underset{\sim}{k}}^{(\alpha)}$ corresponds to a distinct value of α whereas $\underset{\sim}{k}$ is the wavevector corresponding to energy $\mathcal{E}$.

3. (a) Parameter b vs $\log_{10}s$, as it appears in (33).

   (b) Parameter c vs $\log_{10}s$, as it appears in (34).

4. Plots of the distribution $f_o(x)/\Lambda$ for various values of electric field s in the limit $\Lambda << 1$. The optical frequency $\Delta \simeq 2.4$ is shown.

5. Derived values of drift velocity (S-L), compared to experimental values (Jacoboni et al[11]).

6. Monte Carlo (•) and analytic (—) distribution function vs charge-carrier energy for n-type Silicon at 300°K, s = 100 and $\Lambda << 1$.

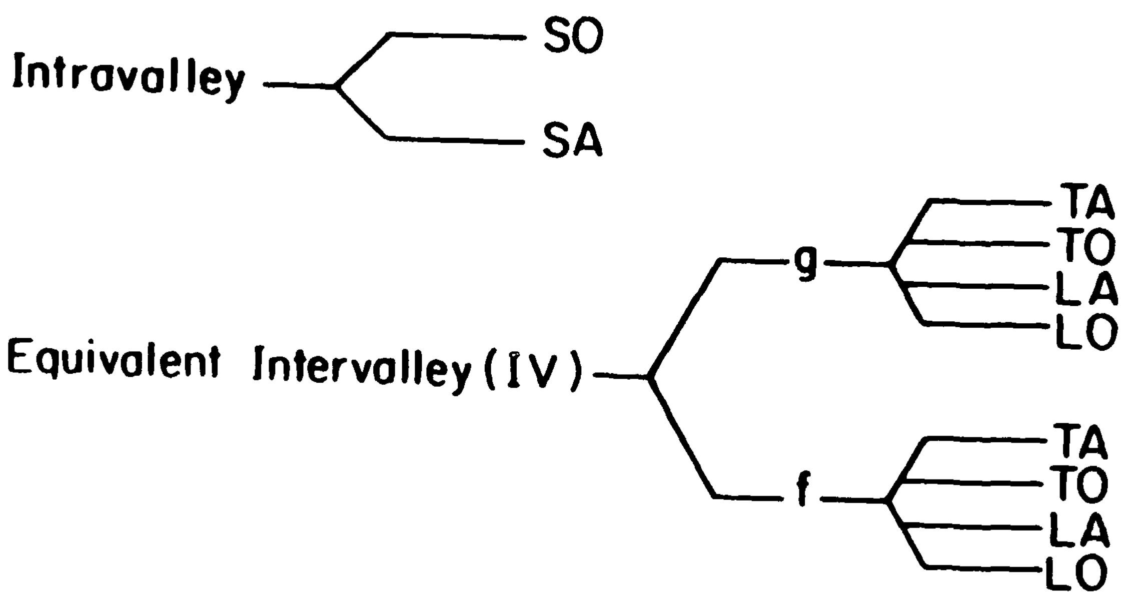
Intravalley
SO
SA
Equivalent Intervalley (IV)
g
TA
TO
LA
LO
f
TA
TO
LA
LO

Figure 1

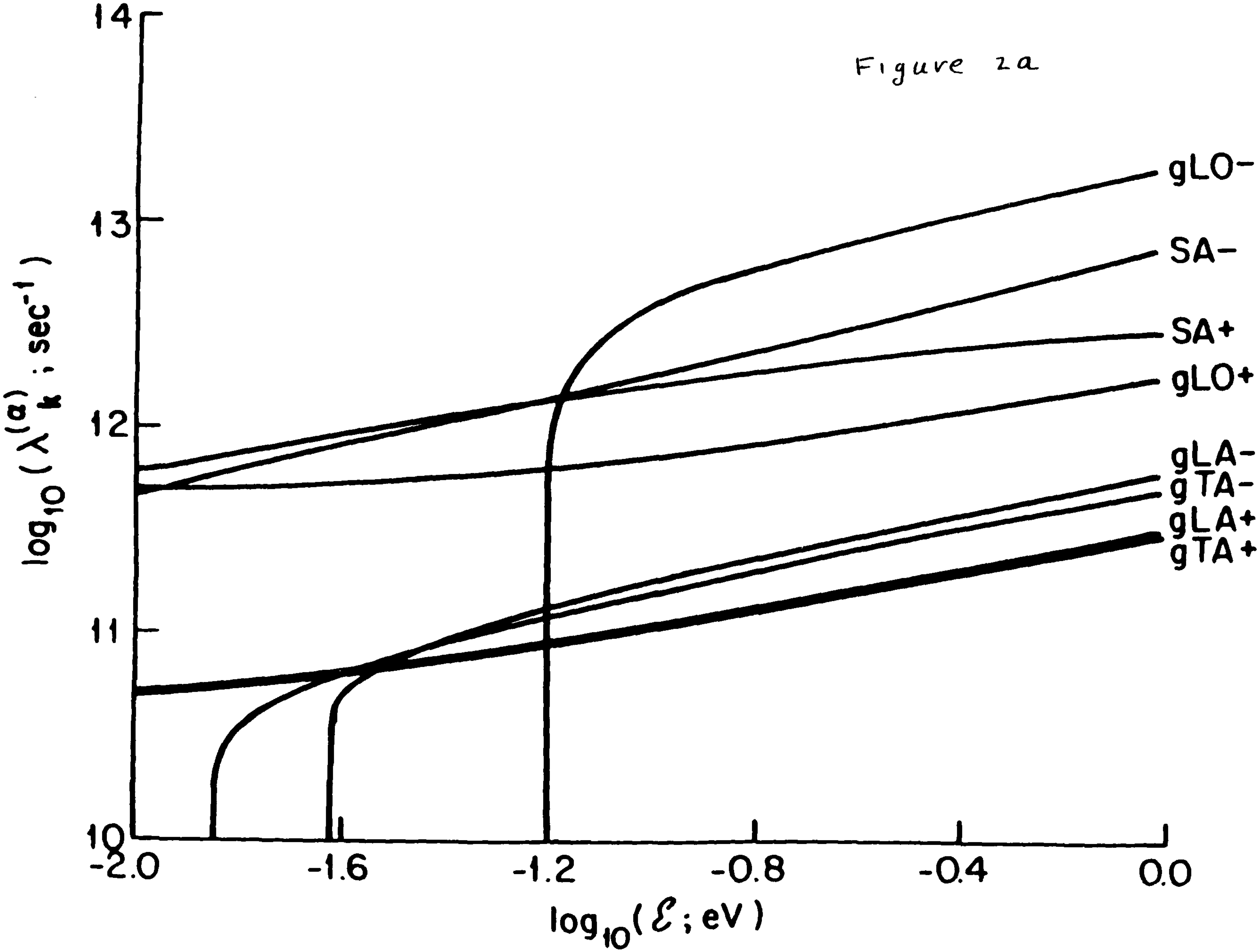
14
13
12
11
10
-2.0
-1.6
-1.2
-0.8
-0.4
0.0
log10(ℰ; eV)
log10(λ(α)k; sec-1)
gLO-
SA-
SA+
gLO+
gLA-
gTA-
gLA+
gTA+

Figure 2a

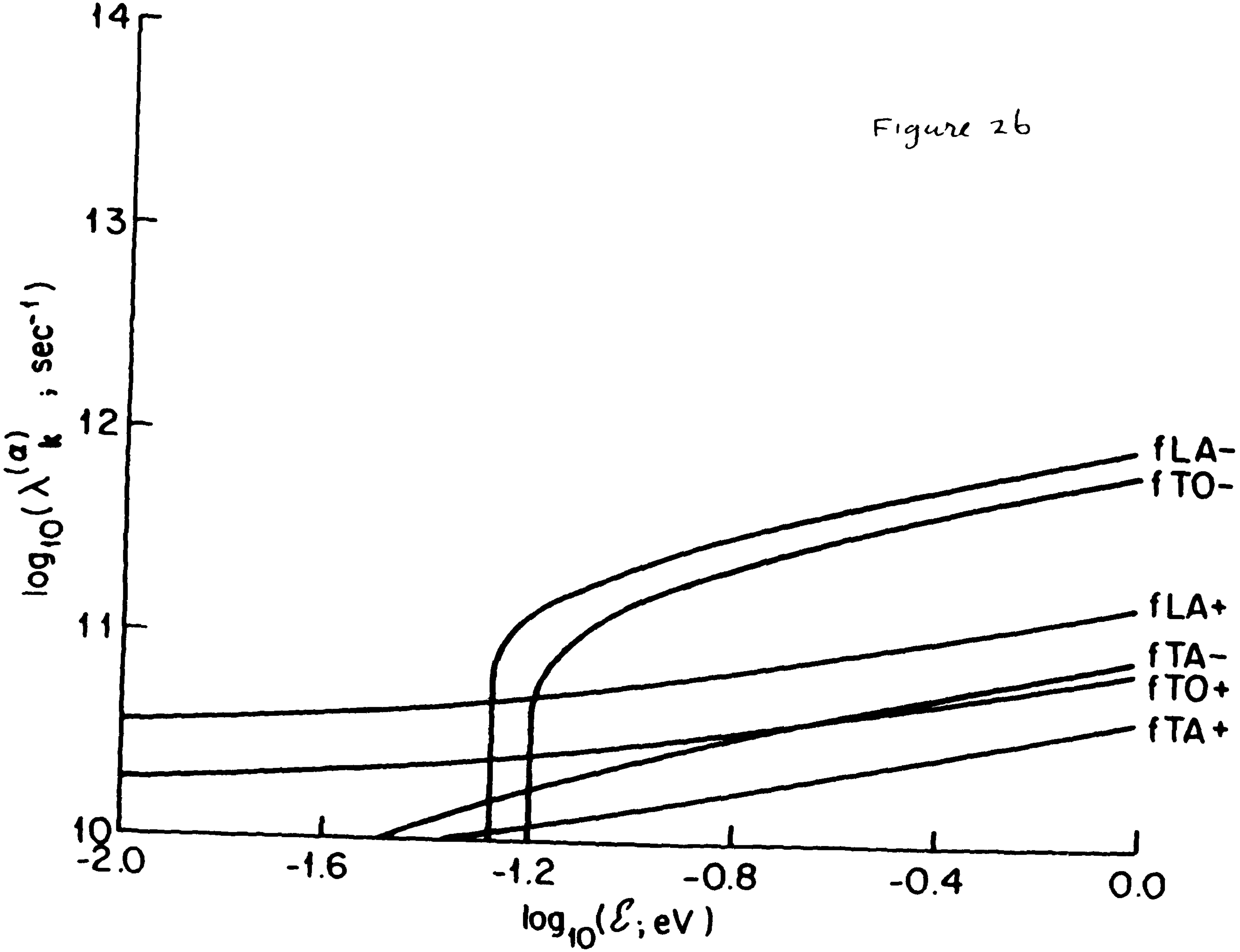

14
13
12
11
10
-2.0
-1.6
-1.2
-0.8
-0.4
0.0
log10(λk(a) ; sec-1)
log10(ℰ; eV)
fLA-
fTO-
fLA+
fTA-
fTO+
fTA+

Figure 2b

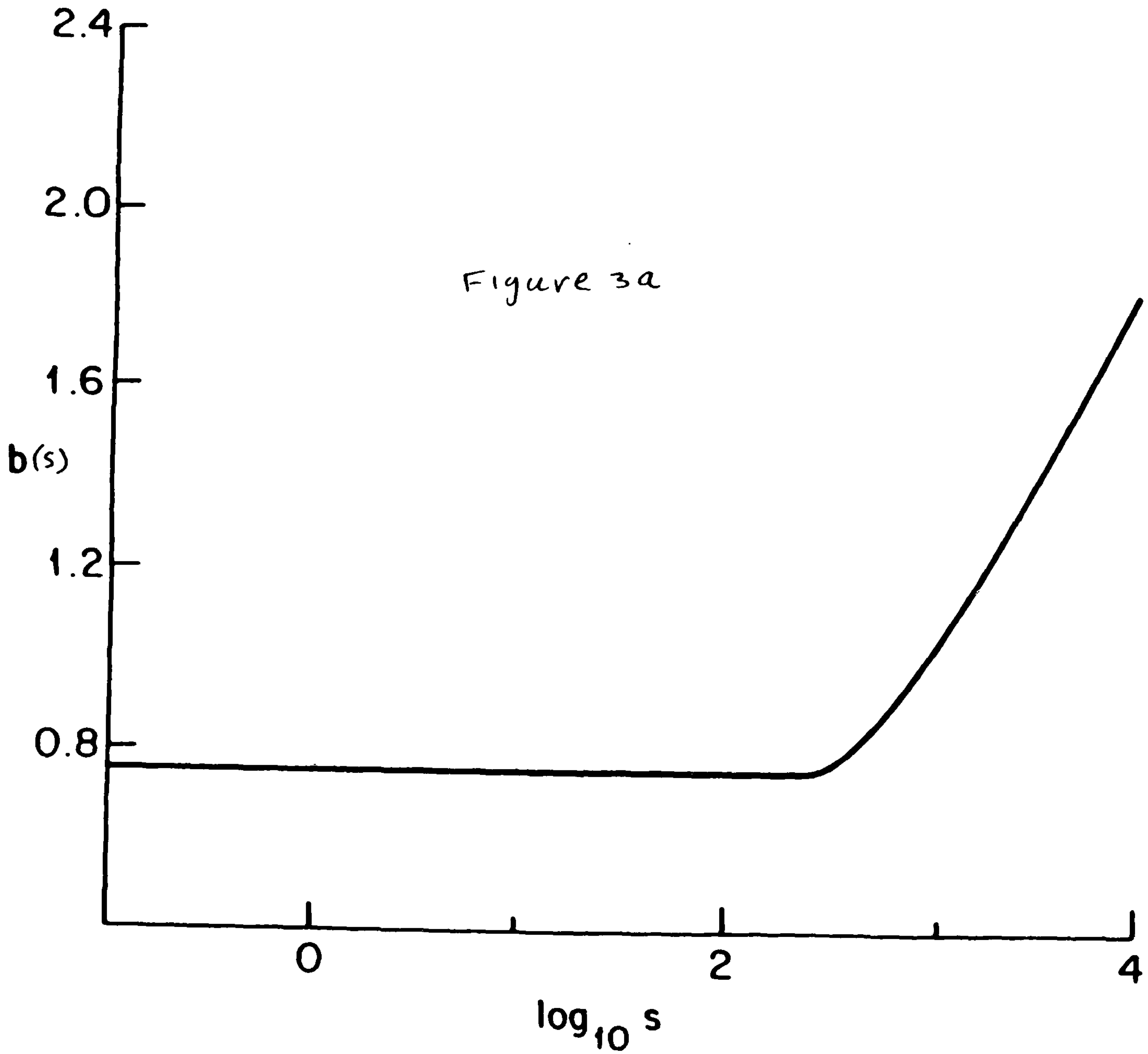

Figure 3a

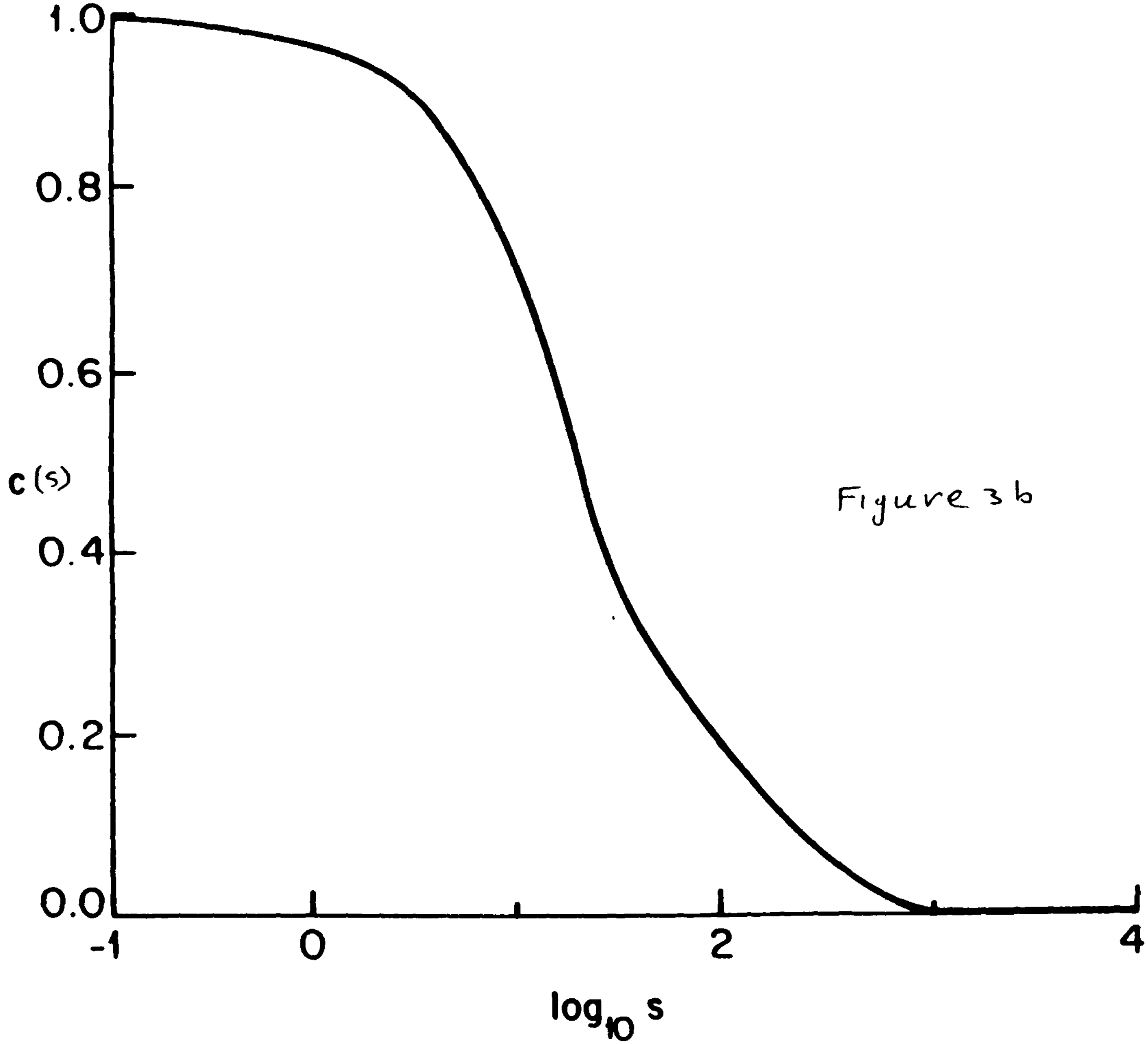

Figure 3b

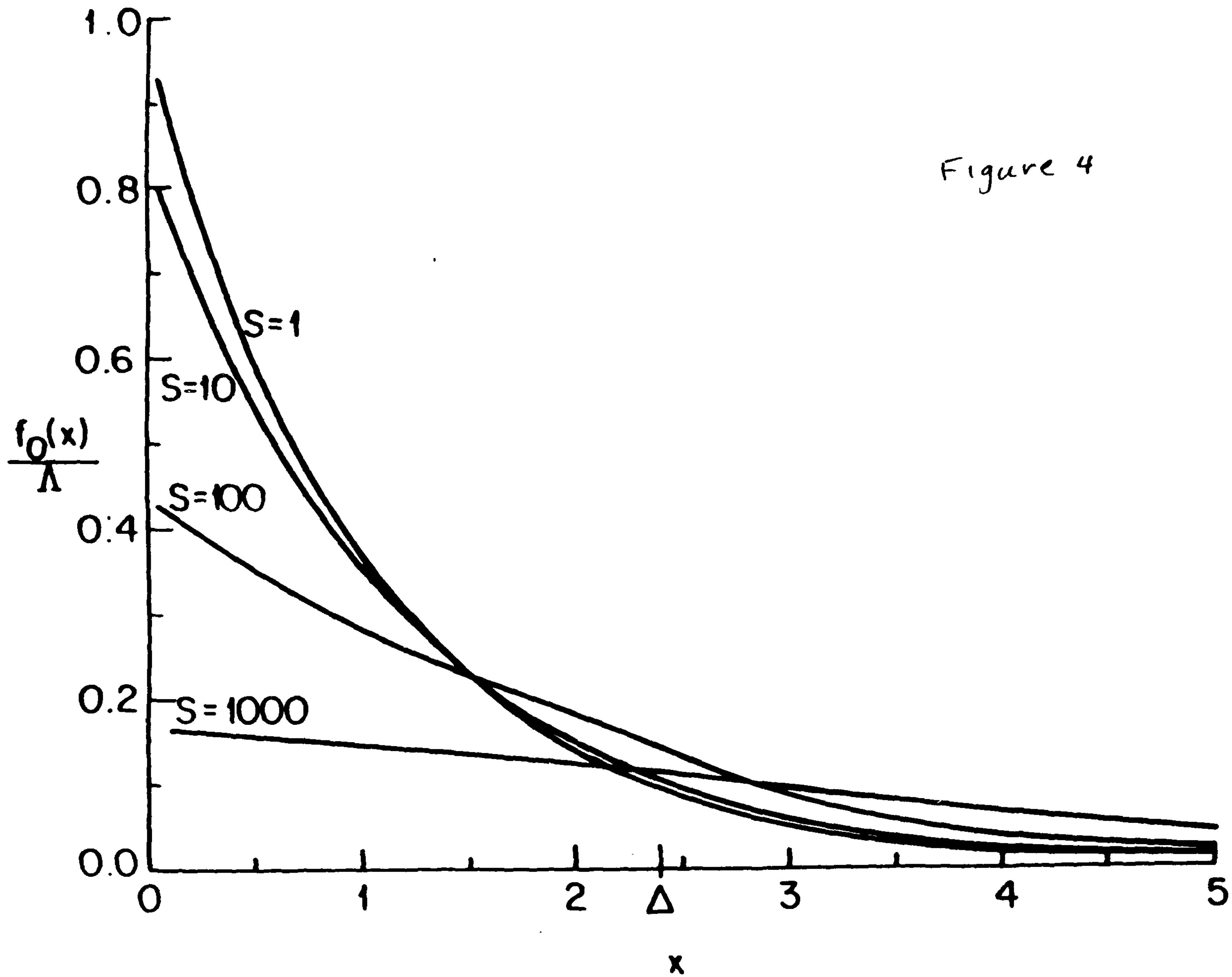

Figure 4

32

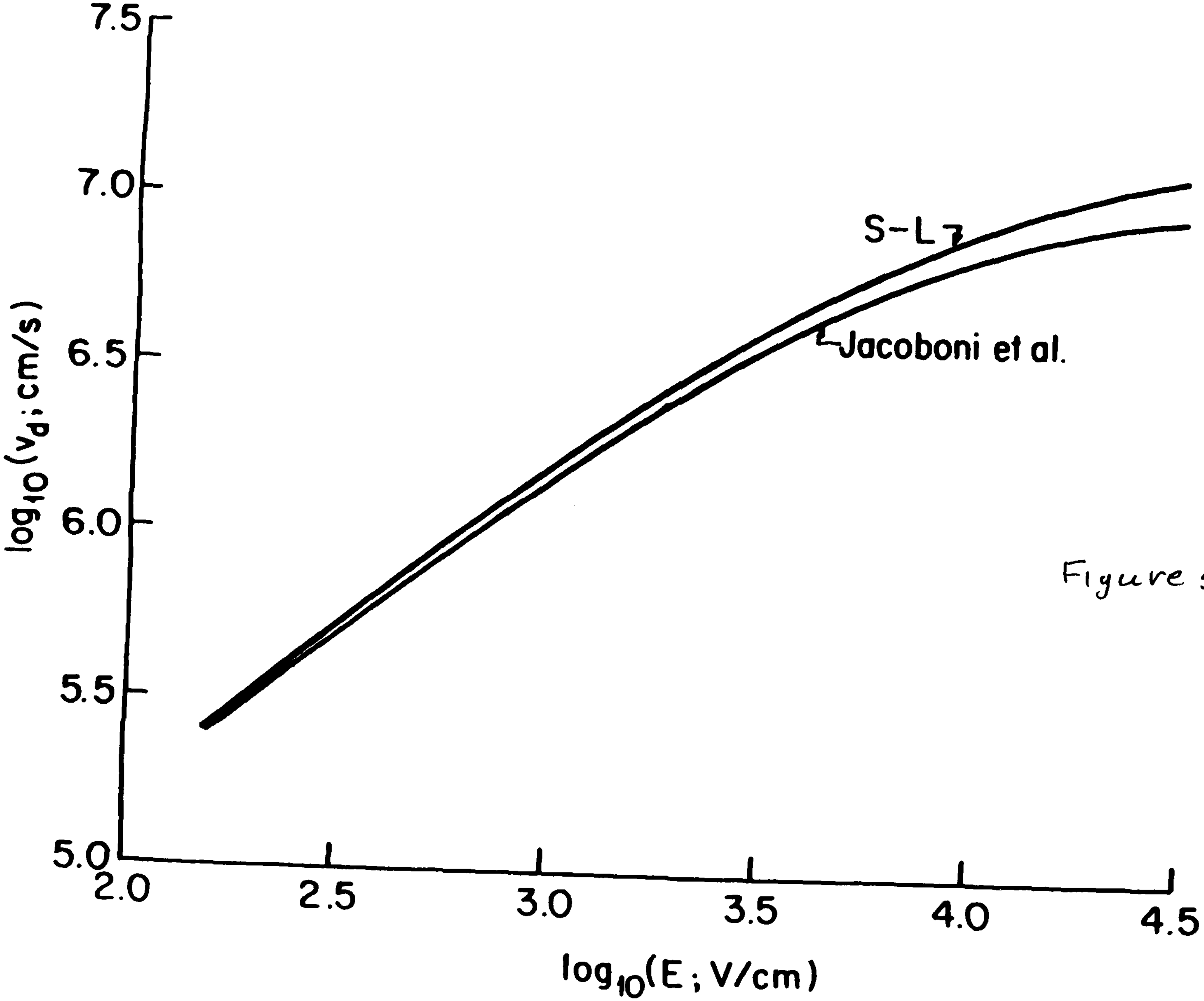

7.5
7.0
6.5
6.0
5.5
5.0
2.0
2.5
3.0
3.5
4.0
4.5
log10(vd; cm/s)
log10(E; V/cm)
S-L
Jacoboni et al.

Figure 5

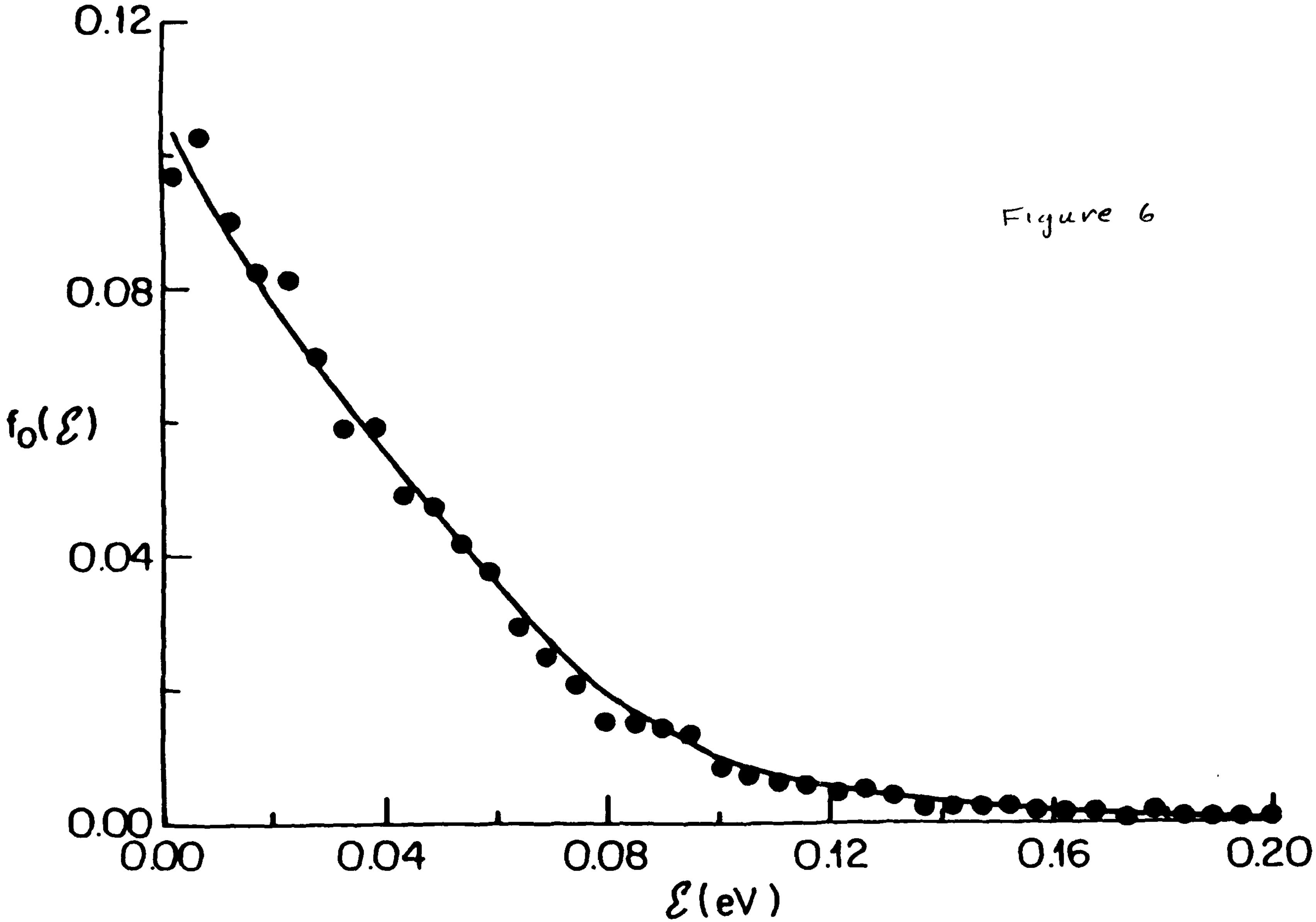

Figure 6